



# Magneto-excitonic states in charge-tunable self-assembled quantum dots

C. Schulhauser<sup>a</sup>, A. Högele<sup>a</sup>, A.O. Govorov<sup>b</sup>, R.J. Warburton<sup>c</sup>, K. Karrai<sup>a,\*</sup>,  
J.M. Garcia<sup>d</sup>, B.D. Gerardot<sup>e</sup>, P.M. Petroff<sup>e</sup>

<sup>a</sup>Center for NanoScience, Sektion Physik, Ludwig-Maximilians-Universität, Geschwister-Scholl-Platz 1, 80539 München, Germany

<sup>b</sup>Department of Physics and Astronomy, Ohio University, Athens, OH, USA

<sup>c</sup>Department of Physics, School of Engineering and Physical Sciences, Heriot-Watt University, Edinburgh EH14 4AS, UK

<sup>d</sup>Instituto de Microelectronica de Madrid, CNM-CSIC Isaac Newton, 8, PTM, 28760 Madrid, Spain

<sup>e</sup>Materials Department, University of California, Santa Barbara, CA 93106, USA

---

## Abstract

The luminescence spectroscopy of charge tunable self-assembled InAs quantum dots is reviewed. We discuss that for confined excitons charged with more than three electrons in excess the quantum dot state can be resonantly coupled to the two-dimensional continuum of electronic states of the wetting layer. This coupling manifests itself in a magnetic field and is triggered by photon emission. In contrast the neutral, singly and doubly charged exciton have optical spectra consistent with the artificial atom picture.

© 2004 Published by Elsevier B.V.

PACS: 73.21.La; 75.75.+a

Keywords: Charged excitons; Semiconductor quantum dots; Single dot spectroscopy; Magnetoluminescence

---

## 1. Introduction

A semiconductor quantum dot is described in terms of artificial atom because the electron and hole confinement leads to discrete energy levels. As the quantum dot is filled either with excitons [1] or with electrons [2,3], shell structure is observed. The long coherence times of an exciton in a quantum dot [4–6] validates the artificial atom picture, motivating the application of quantum dots in

quantum information processing and in quantum optics. For instance, single photon sources exploit the discrete energy levels of a single quantum dot luminescence [7–10]. Further, it has been recently experimentally demonstrated that excitons in quantum dots can be manipulated coherently [11–13]. Recently we demonstrated that when a magnetic field is applied on a multiply charged quantum dots there are electronic states that go beyond the standard artificial atom model [14]. Wojs and Hawrylak [15] pioneered the theory of photoluminescence of multiply charged excitons in magnetic fields as early as 1997. More recently we

---

\*Corresponding author. Fax: +48-89-2180-3182.

E-mail address: [karrai@lmu.de](mailto:karrai@lmu.de) (K. Karrai).

found that the magnetic field induces new states that have no analogue in atomic physics [14]. These states are generated by the emission of a photon from a quantum dot and correspond to a coherent superposition (hybridization) of localized quantum dot states and extended continuum states [1]. As part of a lecture given at the 13th Mauterndorf international winter school on low-dimensional system, we review here the magneto-spectroscopy of charged excitons confined in self-assembled InAs quantum dots.

## 2. Luminescence of charged quantum dots

The generation of excitons with a well defined charge in individual self-assembled quantum dots is obtained in charge tunable field effect structures [2,3]. The quantum dots are embedded in a vertical tunneling structure. An electron–hole pair is photo-generated in the dot with weak optical laser excitation and the electrostatic potential of the dot is controlled through the voltage applied to the gate. The InAs quantum dots are grown in the Stranski–Krastanov mode on GaAs with an annealing step at the growth temperature in order to increase the ensemble photoluminescence energy from 1.1 to 1.3 eV. Under special conditions, the annealing step can lead to the formation of quantum rings. Here, we use the annealing step to form heavily alloyed dots with a lateral height of about 3 nm and a lateral extent of about 40 nm. The heterostructure sequence is GaAs (buffer layer), n+-GaAs (back contact), 25 nm GaAs (tunnel barrier), the quantum dots layer, and 150 nm GaAs/AlAs superlattice (blocking barrier). Contacts are made to the n+ layer and a 5 nm NiCr layer (gate electrode) is deposited on the surface. A voltage  $V_0$  is applied between gate and back contact. The sample is mounted into a homemade titanium miniature cryogenic confocal microscope placed in the 50 mm bore of superconducting magnet capable of producing field ramps ranging from  $-9$  to  $+9$  T cooled to 4.2 K. A unique feature of this microscope is its long-term stability against drifts due to change in temperature and magnetic fields, making it possible to investigate a given single quantum dot

uninterrupted during weeks. The photoluminescence is excited by non-resonant excitation of the wetting layer with a 830 nm laser diode; the photoluminescence is dispersed with a grating spectrometer and detected with a silicon charged-coupled-device camera (spectral resolution 0.1 meV). The excitation power is low enough that any biexciton related features are much weaker than the exciton photoluminescence. The exciton emissions are labeled according to the excess electron charge;  $X^0$  is the neutral exciton,  $X^{1-}$  the negatively charged exciton, and so on. These, as we discuss it below, can be identified unambiguously from the large  $V_g$  extent of the  $X^{1-}$  plateau and the characteristic splitting of the  $X^{2-}$  and the  $X^{3-}$  photoluminescence.

Fig. 1a, shows a plot of photoluminescence from a single dot against gate voltage. The photoluminescence exhibits abrupt shifts in energy at particular values of gate voltage, with plateaus in between. In each plateau, the exciton charge is constant, changing by one electronic charge from one plateau to the next. This is an optical signature of Coulomb blockade [3]. The Coulomb blockade allows us to generate unambiguously an exciton with a particular charge by choosing the gate voltage to lie in the central region of a plateau. The charging luminescence diagram such as shown in Fig. 1 helps us establish the relative magnitude of the single-particle quantization energy and a typical Coulomb energy for the dot studied here. In the Coulomb blockade (Fig. 1), the  $X^{1-}$  plateau extends over a much larger range of gate voltage than the  $X^0$  and  $X^{2-}$  plateaus. The reason for this is that on going from  $X^{1-}$  to  $X^{2-}$ , the higher energy electron orbital, namely the p-orbital, must be occupied (Fig. 2). The width of the  $X^0$  plateau is determined by the Coulomb charging energy required to place a second electron in the already occupied s-orbital; the width of the  $X^{1-}$  plateau in contrast is determined by a similar Coulomb energy plus the quantization energy that separates the p- and the s-orbitals. We can therefore conclude from the length of the plateaus along  $V_g$  that the quantization energy is larger than the Coulomb energy. We describe therefore the charged excitons by treating the Coulomb interactions as perturbations to the single-particle

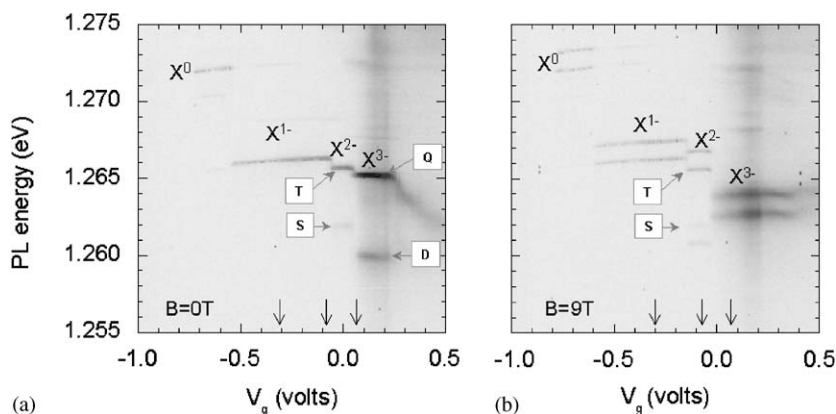


Fig. 1. Photoluminescence versus gate voltage from a single quantum dot at 4.2 K and at zero magnetic fields (a), and at 9 T (b). The photoluminescence (photoluminescence) is represented with a gray-scale. The exciton emissions are labeled according to the excess charge;  $X^0$  is the neutral exciton,  $X^{1-}$  the charged exciton, and so on. These can be identified unambiguously from the large  $V_g$  extent of the  $X^{1-}$  plateau and the characteristic splitting of the  $X^{2-}$  photoluminescence. The arrows mark the  $V_g$  for the measurements in magnetic field.

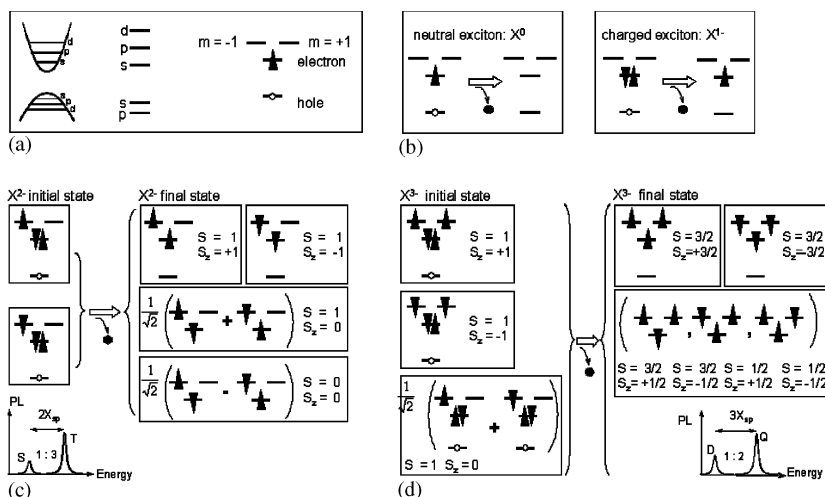


Fig. 2. Quantum dot level diagrams in the artificial atom model. Panel (a) defines the orbitals and symbols. Only the lowest energy hole orbital, labeled s, is shown as only this hole orbital participates in the recombination. The electron orbitals are labeled s and p with z-component of angular momentum  $m = 0; \pm 1$ , respectively. Electrons are shown as arrow heads according to their z-component of spin; the hole has spin  $\pm \frac{3}{4}$ . Panels (b), (c) and (d) shows configurations for the initial and final states of the neutral, singly doubly and triply charged exciton  $X^{3-}$  (with spin  $S=1$  for  $X^{3-}$ ).

states [21]. Information on the single-particle states is obtained from the optical measurements. The quantization energy separating the ground s-orbital and the excited p-orbitals is deduced to be 34 meV from diamagnetic shift measurements [16]. Furthermore, we know that the two p-orbitals are close to degenerate for the dot in Figs. 1 and 2

both from the form of the  $X^{3-}$  photoluminescence at  $B=0$  (explained below) and from the very small fine-structure splitting of the  $X^0$ . We have measured the absorption spectrum with high spectral resolution [17] and we find that the  $X^0$  absorption consists of two orthogonal and linearly polarized lines just 20  $\mu\text{eV}$  apart [17]. This splitting arises

from the anisotropic electron–hole exchange interaction. The isotropic exchange interaction is much larger,  $400 \mu\text{eV}$  [18]. Finally, the d-orbitals cannot exist in our dots as the  $X^{3-}$  is the most highly charged exciton we can generate; at more positive gate voltages, charge occupies not the dot but the wetting layer, as proven by Shubnikov-de Haas oscillations in the device’s capacitance. For values of  $V_g$  ranging from  $+0.12$  to  $+0.5$  V the measured electron density in the wetting layer increased linearly from 0 to  $3 \times 10^{11}/\text{cm}^2$ . It is important to realize that all optical measurements reported in this work are performed for gate values  $V_g < 0.1$  V, meaning that at all times the wetting layer continuum was always empty of electrons.

The  $X^{3-}$  emission process within the strong confinement scheme, and also the artificial atom model, is displayed in Fig. 2. Here we consider only localized quantum dot states. The  $X^{3-}$  initial state has a spin  $S=1$  consistent with Hund’s rule. The two electrons in the upper  $p^-$ - and  $p^+$ -orbitals have lowest energy with parallel spins. When a photon is emitted, there are two final states with  $S = \frac{3}{2}$  and  $S = \frac{1}{2}$ , energetically distinct because of the exchange interaction. This is the origin of the two lines Q and D seen in Fig. 1a in the  $X^{3-}$  emission, the higher (lower) energy line

corresponding to emission into the final quadruplet

$S = \frac{3}{2}$  (doublet  $S = \frac{1}{2}$ ) state as depicted in Fig. 2.

### 3. Magneto-optics of charged quantum dots

As discussed above, the Coulomb blockade allows us to generate an exciton with a particular charge. This property persists in high magnetic fields. Fig. 1b shows photoluminescence from the same dot at a magnetic field of 9 T applied perpendicular to the sample surface along the growth direction. Each luminescence line is now split into two through the spin Zeeman effect, but the Coulomb blockade is retained with the magnetic field inducing only small shifts in the charging voltages. This allows us to measure the magnetic dependency of various charged excitons all on the same dot and will be discussed in the next paragraph. The Neutral exciton has a bright and a dark state that are split from each other by the electron–hole exchange energy  $X_{eh}$ . The dark exciton cannot decay by emitting a photon of angular momentum  $+1$  or  $-1$  because its  $\frac{1}{2}$ -electron and  $\frac{3}{2}$ -hole spin are aligned so that the total exciton spin is  $+2$  or  $-2$ . Two electrons and

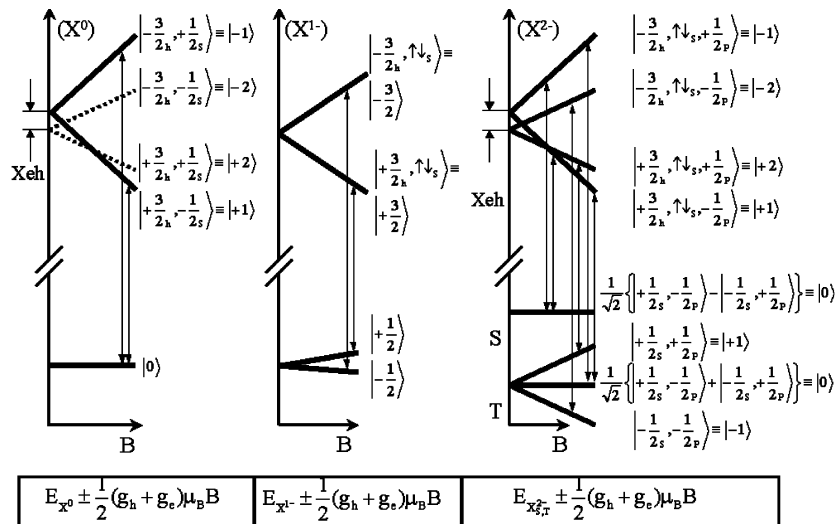


Fig. 3. Allowed optical transition for the neutral ( $X^0$ ), simply charged and doubly charged excitons. In the description of the quantum states, the fractions indexed “h” indicates the spin of the hole and those with index “e” corresponds to that of the electron.

a hole form the singly charged exciton  $X^{1-}$ . The two electrons spin are opposite in accordance with the Pauli principle so that in the  $X^{1-}$  charge configuration there is not net electron–hole exchange energy involved. The doubly charged exciton allows for electron–hole exchange but contrary to the  $X^0$  exciton there is no dark configuration of the exciton and the electron–hole exchange can be measured [18]. All configurations of the  $X^{2-}$  are bright because, as it is depicted in Fig. 3, there is always an optical transition that involves a change in angular momentum of  $+1$  or  $-1$ , a condition necessary to preserve angular momentum in photon emission. This is manifested in the appearance of a fine structure in the emission peak of the  $X^{2-}$  exciton. Although fine structures due to electron–hole exchange are not resolved in the spectra presented in this work we have reported and discussed them elsewhere [18]. In contrast to the situation for electron–hole, the electron–electron exchange energy the doubly and triply charged exciton is large and leads to two well-resolved emission lines for  $X^{2-}$  and  $X^{3-}$  as seen in Fig. 1a. In absence of magnetic field, the split emission lines correspond to the singlet and triplet configuration of the quantum dot after photon emission from the  $X^{2-}$  exciton [3] as it shown in Fig. 2. For the triply charged quantum dots, the electronic configurations after photon emission are that of the quadruplet and doublet states also shown in Fig. 2. The situation in high magnetic field is different. A careful inspection of Fig. 1b shows that the splitting originating from the electron–electron exchange persists at high magnetic field for the  $X^{2-}$  but has disappeared for the  $X^{3-}$ .

Fig. 3 shows the expected magnetic Zeeman dispersions of the neutral exciton  $X^0$ , the singly charged exciton,  $X^{1-}$  and the doubly charged exciton,  $X^{2-}$  along with the allowed optical transitions. The selection rules for the optical transitions involve a change in angular momentum of  $+1$  or  $-1$ . In the presence of a magnetic field, all allowed optical transitions split in two Zeeman emission lines. For  $X^0$ ,  $X^{1-}$ , and  $X^{2-}$ , the excitonic Zeeman splitting is given by the sum of the hole and electron Zeeman splitting  $(g_h + g_e)\mu_B B$  irrespective of the charge in the dot. This is a consequence of the change in angular momentum  $\pm 1$  required upon photon emission. In the Faraday geometry the optical wave vector for optical emission is parallel to the applied magnetic field and the dark exciton in  $X^0$  remains dark at all magnetic fields.

Fig. 4 shows the measured dispersion of the photoluminescence for the singly, doubly and triply charged exciton. For the neutral exciton  $X^0$  (not shown here), the charged  $X^{1-}$  and the doubly charged  $X^{2-}$  excitons the magnetic dispersion is typical of strongly localized bound electron–holes complexes [16]. The luminescence line splitting is linear in  $B$  and arises from the spin Zeeman effect [16]. A diamagnetic shift, quadratic in magnetic field  $B$ , originating from the enhancement of the exciton confinement is also clearly seen [16]. The corresponding allowed magneto optical transitions are shown in Fig. 2. As expected for the allowed transitions shown in Fig. 3, the exciton Zeeman energy splitting remains independent on the charge. The  $X^{2-}$  photoluminescence has two lines at zero magnetic field as a consequence of

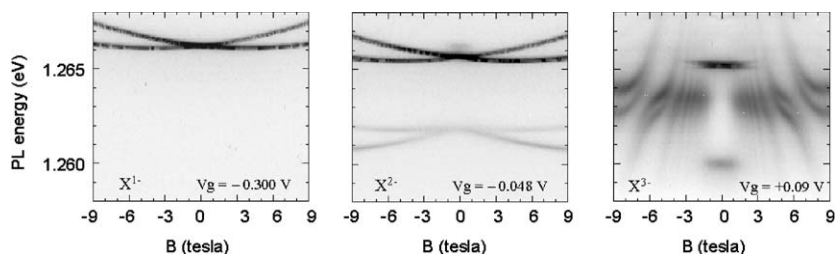


Fig. 4. Measured photoluminescence emission of excitons confined in the same single quantum dot as function of their charge. From left to right: one, two and three electrons in excess. The measurements are represented with a grey scale and were performed at constant gate voltage shown in the figures and shown arrows in Fig. 1. The temperature was 4.2 K.

exchange-split final states, one with  $S=1$ , the other with  $S=0$  as it can be seen in Fig. 2. There is a slight difference between the  $X^{1-}$  and  $X^{2-}$  dispersions in magnetic field. We need to introduce a small term proportional to  $|B|$  to fit the  $X^{2-}$  energy dispersion, but not the  $X^{1-}$  or  $X^0$  dispersion. We tentatively ascribe this to an interaction with the nuclear spins. It is known that under certain conditions, a circularly polarized optical excitation (which we employ here) can lead to a polarization of the nuclei, unaffected by the charging state of the dot.

The triply charged exciton  $X^{3-}$  in contrast has a dramatically different behavior. At low fields, a gradual collapse around 1 T of the quadruplet and doublet spectral lines into a single line. At high field, the photoluminescence develops a remarkable series of oscillations in addition to the spin Zeeman effect [14]. This behavior was observed for  $X^{3-}$  on all dots studied so far. Using the artificial atom model we explain the low field collapse of the  $X^{3-}$  doublet and quadruplet lines into a single broad line [14]. The applied magnetic field introduces an orbital Zeeman splitting between the two  $p^-$  and  $p^+$ -orbitals [19]. For a two-dimensional parabolic quantum confinement, the orbital Zeeman splitting is given by the cyclotron energy  $\eta\omega_c = \eta eB/m^*$  [19,21]. When the splitting between the  $p$ -orbitals exceeds the exchange energy, both  $p$ -electrons occupy the lower energy  $p^-$ -orbital and form an  $S=0$  initial state for the  $X^{3-}$  exciton [20] as this configuration becomes energetically favorable. The collapse of the photoluminescence splitting around 1 T is a signature for this change in configuration. Two arguments show this. First, the field at which the configuration change occurs can be determined from the splitting in the photoluminescence at zero fields. For a harmonic confining potential, the exchange interaction energy between two  $p$ -electrons  $X_{pp}$  is  $X_{pp} = \frac{3}{4} X_{sp}$  [21], and the magnetic field induces a splitting of  $\eta\omega_c$  between the  $p$ -orbitals [21]. The energy  $X_{sp}$ , the exchange energy between an  $s$ - and a  $p$ -electron, is experimentally determined from the energy separating the triplet and the singlet line  $\Delta E_{TS} = 2X_{sp}$  or equivalently from the energy splitting between the doublet and the quadruplet line  $\Delta E_{DQ} = 3X_{sp}$  [3]. Hence, the configuration

change occurs when  $\eta\omega_c = \Delta E_{DQ}/4$ , corresponding to a magnetic field of 0.8 T (taking an effective mass of  $m^* = 0.07$ ), a value in agreement with the experimental results. Secondly, once the triply charged exciton  $X^{3-}$  forms an initial  $S=0$  state, there is only one possible final state energy. The photoluminescence line therefore “collapses” and its energy is located in between the two exchange-split lines of the  $S=1$   $X^{3-}$  emission. This exactly what is observed in Fig. 1b and in Fig 4. Within this artificial atom picture however, there is no explanation for the series of the level-repulsion that develop at higher magnetic field. The high field behavior can only be interpreted with a new electronic interaction.

The series of anti-crossings can be clearly seen in Fig. 5. We concluded that an interaction with Landau levels is responsible for this behavior [14]. The asymptotes at each anti-crossing are linear functions of magnetic field and all of them extrapolate back to the same energy at zero magnetic field. Both of these features are characteristic of Landau levels. Furthermore, the  $X^{3-}$  luminescence intensity at constant energy is a periodic function of  $1/B$ . Such behavior is well known not in quantum dot optics but rather in the properties of conducting two-dimensional systems. The surprising result is that the photoluminescence from an exciton bound to a small quantum dot takes on the properties of extended states at much higher energies, the Landau levels. The

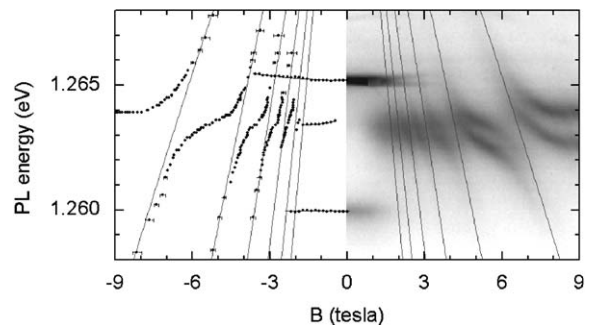


Fig. 5. Position of luminescence maxima for the  $X^{3-}$  exciton. In the plot on the left we plot the upper spin branch of the emission measured in the left part of the plot. The asymptotic branches are the best fit to Landau levels coupled to the final state. The gray scale corresponds to the data shown in Fig. 4 for a gate voltage of 0.09 V.

anti-crossings in Fig. 5 prove that the quantum dot interacts coherently with the Landau levels. For instance, from the splitting at the 6.5 T resonance (2.4 meV), we can deduce that the system oscillates between localized quantum dot character and Landau level character with a frequency of 0.6 THz. The asymptotes shown in Fig. 3 have a negative slope. Bearing in mind that a photoluminescence experiment measures the energy difference between two states, the initial state and the final state depicted for instance in Figs. 2 and 6, the negative dispersion demonstrates that the hybridization takes place in the final state. In other words, photon emission triggers the hybridization, a point that is central to the new electronic interaction revealed in this experiment [14].

Quantum mechanical configurations with the same good quantum numbers and similar energies are admixed. This is a manifestation of the indistinguishable nature of electrons through Coulomb interaction. For the  $S=1$  initial state of  $X^{3-}$ , and also the doubly charged exciton  $X^{2-}$ , the final state configurations involve only the s- and p-orbitals. However, we find a new possibility for the final state of the  $S=0$  initial state of  $X^{3-}$  which has a doubly occupied p-orbital and a singly occupied s-orbital. In this case, the quantum numbers are preserved by allowing one of the p-electrons to fill the vacancy in the s-orbital, with the other p-electron occupying a

higher energy in the wetting layer two-dimensional continuum of states. These two configurations, not only have the same values of angular momentum and spin but are also almost degenerate, and therefore the final state is an admixture of the two. This means that the state occupied by the electron in continuum inevitably imparts its character to the photoluminescence even though it is never occupied in the initial state. For our dot potential, the d-orbital is unbound and this why the hybridization mechanism now admixes *continuum* states to the quantum dot wave function, [14], as shown in Fig. 6. The continuum states are associated with the two-dimensional wetting layer. In a magnetic field, the continuum states are quantized into Landau levels, such that the final state becomes a hybridization of quantum dot states and Landau levels. In this model, the hybridization occurs for the  $S=0$   $X^{3-}$  exciton but not for the  $S=1$   $X^{3-}$  or the more weakly charged excitons. There is therefore a close correspondence with the experiments, where the  $S=0$   $X^{3-}$  interacts with the Landau levels but the other excitons do not. Additionally, the interaction takes place in the final state, as we deduced from the asymptotes to negative slopes. In a magnetic field, the exciton final state is strongly hybridized whenever the energy between the occupied p<sup>-</sup>-orbital and the s-orbital exactly matches the energy between a particular Landau level and the p<sup>-</sup>-orbital, as shown in Fig. 6. This implies that

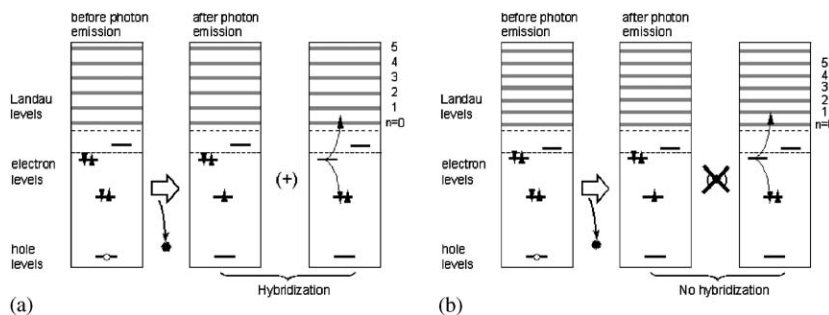


Fig. 6. At high enough magnetic fields, the initial state of  $X^{3-}$  is in the  $S=0$  configuration. Exciton optical transition diagrams showing the two possible configuration state in which the exciton can decay in. After photon emission one of the two possible states has an electron in the continuum of state of the wetting layer. In case (a) the energy of electron in the continuum energy matches that of a Landau level. Both states are equally accessible so hybridization occurs. In (b) the magnetic field is modified (here reduced) so that the higher electron energy falls in a gap in the density of state between two Landau levels. Only the state in which the two electrons are left in the p-state are accessible so hybridization is inhibited. The hybridization is turned on and off periodically in  $1/B$ .

hybridization with the  $n$ th Landau level occurs when  $\Delta = (n + 3/2)\eta\omega_c$  where  $\Delta$  is the excess kinetic energy (at  $B=0$ ), defined as the difference in energy between the electron in the continuum and band edge energy (at  $B=0$ ). (We have assumed that the  $p^-$ -orbital moves down in energy by  $\eta\omega_c/2$  and the  $p^+$ -orbital moves up by  $\eta\omega_c/2$ , an exact result for a harmonic confinement [19]). As the magnetic field is increased, this condition is satisfied for each Landau level in turn, resulting in the periodicity in  $1/B$ . For the dot presented in this work, we find that the excess kinetic energy of the higher energy electron is  $\Delta = 20$  meV. The mechanism we propose for the hybridization conserves angular momentum. Hybridization with every Landau level is always allowed because every Landau level has all orbital components independent of the Landau level index [22]. Ultimately, at high magnetic field, the interaction with the Landau levels is suppressed because the separation between the  $s$ - and  $p^-$ -orbitals becomes insufficient. We reach this regime at  $B \gg 8$  T for our particular dot. When there is a resonance with a Landau level, the hybridization leads to two states, split in energy by twice the interaction matrix element. To confirm that our mechanism can account quantitatively for the experimental results, we have calculated Coulomb interaction matrix element using harmonic oscillator wave functions, and Landau level wave functions in the symmetric gauge [22] centered on the dot. We find an analytical expression for the splitting between the photoluminescence lines [14] amounting to 2.0 meV for our quantum dots in very good agreement with the experimental result, namely 2.4 meV. Additionally, we find that the  $S=1$  configuration of  $X^{3-}$  cannot couple to the continuum through this mechanism, exactly as observed in the experiment. The physics we are describing here is a novel interaction between a localized state and a continuum at higher energy [14]. It is worth pointing out that for extended states, analogous photon triggered configuration mixing where found in the excitonic emission from a high mobility two dimensional electron systems [23]. To obtain a quantitative description we have developed a new version of the Anderson/Fano model in order to describe the emission properties

of the final state with a filled continuum. The details of this work are discussed elsewhere [14,24]. We anticipate that the interaction between the quantum dot state with a continuum filled with electrons allows for the possibility of new Kondo-like effects [24] because there can be a coherent interaction between localized and delocalized electrons [25].

Information on the exact nature of the Landau levels can be obtained by analyzing the data in Fig. 5. According to the model, there are two bare final states as shown in Fig. 6. The first involves two electrons in  $p^-$  and one electron in the  $s$ -level with emission energy,  $E_0$ . The second has two electrons in the  $s$ -level and one electron in the continuum with energy  $E_1$ . The energy  $E_0$  is independent of magnetic field (neglecting the small diamagnetic shift), whereas  $E_1 = E_0 + \Delta - (n + 3/2)\eta\omega_c$ . The hybridization introduces anti-crossings between  $E_0$  and  $E_1$ . For a coupled two-level system, far away from an anti-crossing, the hybridized state follows very closely either one energy or the other. We use this to fit the form of  $E_1$  to the asymptotes in Figs. 4 and 5. We find that the fit is adequate for a constant effective mass,  $m^*$ , but is perfect if we allow  $m^*$  to depend slightly on magnetic field according to  $m^* = 0.07 - 0.0018|B| + 0.00005 B^2$  with  $E_0 = 1,2635$  eV and  $\Delta = 20$  meV. We note that inclusion of the diamagnetic shift in the analysis does not change the masses we deduce significantly. The mass therefore decreases with magnetic field; equivalently, it decreases at constant energy with decreasing Landau level index  $n$ . This is both opposite in sign and larger in magnitude than the changes associated with band non-parabolicity. We suggest the following explanation. At the resonance with a large  $n$  Landau level, the field is small and so the Landau level is much more extended than the dot such that the mass is typical to that of the wetting layer. Conversely, at the resonance with the  $n=0$  Landau level, the Landau level is much more localized, and the mass is reduced by the indium content of the dot. For example, the resonance with the  $n=4$  Landau level takes place when the spatial extent of the Landau level is 105 nm; the corresponding length for the  $n=0$  at resonance is just 20 nm. We note that this measurement provides a very sensitive probe of the

details of these continuum-like states that have not been characterized previously.

In summary, we have reviewed the physical properties of charged excitons confined in a self-assembled quantum dot, showing that the optical emission of such excitons can be used to probe the energy continuum located well above the confined electronic energies. The central point in our findings is that a vacancy in the s electron orbital is a necessary condition to obtain the hybridization with the continuum. Such a vacancy is generated after optical emission, meaning that it is the photon emission that forces hybridization between localized and extended states to take place. It is essential to appreciate that the interaction with the continuum in magnetic field is not a source of scattering but is instead coherent. A signature of the coherent behavior is the anticrossings that are seen in the optical emission. This photon-triggered hybridization is not unique to our particular quantum dots. The interaction should be a feature for more highly charged excitons because after photon emission, there is a vacancy in the s-orbital with a filled p-orbital. For deeper dot potentials where the d-orbital is bound, the interaction will admix d character, but ultimately for the most highly charged excitons such a dot can support, the exciton energy will lie just below the continuum such that hybridization with the continuum takes place. Only shallow dots which can accommodate no more than two electrons are unaffected by the hybridization. In other words, the hybridization we propose here is significant for almost all self-assembled quantum dots.

Future perspective for this work is to investigate the nature of interaction between the electronic localized wave functions in the dot with a two-dimensional delocalized electron system filling the continuum of the wetting layer [24,25].

## Acknowledgements

We acknowledge stimulating discussions with Achim Rosch and Jan von Delft. This work was funded by the DFG SFB 348, EPSRC and The Royal Society.

## References

- [1] M. Bayer, O. Stern, P. Hawrylak, S. Fafard, A. Forchel, *Nature* 405 (2000) 923.
- [2] H. Drexler, D. Leonard, W. Hansen, J.P. Kotthaus, P.M. Petroff, *Phys. Rev. Lett.* 73 (1994) 2252.
- [3] R.J. Warburton, C. Schäfflein, D. Haft, F. Bickel, A. Lorke, K. Karrai, J.M. Garcia, W. Schoenfeld, P.M. Petroff, *Nature* 405 (2000) 926.
- [4] D. Gammon, E.S. Snow, B.V. Shanabrook, D.S. Katzer, D. Park, *Science* 273 (1996) 87.
- [5] P. Borri, W. Langbein, S. Schneider, U. Woggon, R.L. Sellin, D. Ouyang, D. Bimberg, *Phys. Rev. Lett.* 87 (2001) 157401.
- [6] M. Bayer, A. Forchel, *Phys. Rev. B* 65 (2002) 041308.
- [7] P. Michler, A. Kiraz, C. Becher, W. Schoenfeld, P.M. Petroff, L. Zhang, E. Hu, A. Imamoglu, *Science* 290 (2000) 2282.
- [8] E. Moreau, I. Robert, L. Manin, V. Thierry-Mieg, J.M. Gérard, I. Abram, *Phys. Rev. Lett.* 87 (2001) 183601.
- [9] Z. Yuan, B.E. Kardynal, R.M. Stevenson, A.J. Shields, C.J. Lobo, K. Cooper, N.S. Beattie, D.A. Ritchie, M. Pepper, *Science* 295 (2001) 102.
- [10] C. Santori, D. Fattal, J. Vučković, G.S. Solomon, Y. Yamamoto, *Nature* 419 (2002) 594.
- [11] N.H. Bonadeo, J. Erland, D. Gammon, D. Park, D.S. Katzer, D.G. Steel, *Science* 282 (1998) 1473.
- [12] H. Kamada, H. Gotoh, J. Temmyo, T. Takagahara, H. Ando, *Phys. Rev. Lett.* 87 (2001) 246401.
- [13] A. Zrenner, E. Beham, S. Stuffer, F. Findeis, M. Bichler, G. Abstreiter *Nature* 418 (2002) 612.
- [14] K. Karrai, R.J. Warburton, C. Schulhauser, A. Högele, B. Urbaszek, E.J. McGhee, A.O. Govorov, J.M. Garcia, B.D. Gerardot, P.M. Petroff, *Nature* 427 (2004) 135.
- [15] A. Wójs, P. Hawrylak, *Phys. Rev. B* 56 (1997) 13227.
- [16] C. Schulhauser, D. Haft, R.J. Warburton, K. Karrai, A.O. Govorov, A.V. Kalameitsev, A. Chaplik, W. Schoenfeld, J.M. Garcia, P.M. Petroff, *Phys. Rev. B* 66 (2002) 193303.
- [17] B. Alèn, F. Bickel, K. Karrai, R.J. Warburton, P.M. Petroff, *Appl. Phys. Lett.* 83, 2003; 2325. A. Högele, S. Seidel, M. Kroner, R.J. Warburton, K. Karrai, B.D. Gerardot, P.M. Petroff, submitted for publication 2004.
- [18] B. Urbaszek, R.J. Warburton, K. Karrai, B. Gerardot, P.M. Petroff, J.M. Garcia, *Phys. Rev. Lett.* 90 (2003) 247403.
- [19] V. Fock, *Z. Phys.* 47 (1928) 446.
- [20] S. Tarucha, D.G. Austing, T. Honda, R.J. van der Hage, L.P. Kouwenhoven, *Phys. Rev. Lett.* 77 (1996) 3613.
- [21] R.J. Warburton, B.T. Miller, C.S. Dürr, C. Bödefeld, K. Karrai, J.P. Kotthaus, G. Medeiros-Ribeiro, P.M. Petroff, S. Huant, *Phys. Rev. B* 58 (1998) 16221.
- [22] R.B. Dingle, *Proc. R. Soc. A* 211 (1951) 500.
- [23] L. Gravier, M. Potemski, P. Hawrylak, B. Etienne, *Phys. Rev. Lett.* 80 (1998) 3344.
- [24] A.O. Govorov, K. Karrai, R.J. Warburton, *Phys. Rev. B* 67 (2003) 241307R.
- [25] A.C. Hewson, *The Kondo Problem to Heavy Fermions*, Cambridge University Press, Cambridge, 1993.